Distillation Absorption 2010
A.B. de Haan, H. Kooijman and A. Górak (Editors)

A STUDY ON SIEVE TRAY LOWER OPERATING LIMIT

Ali Zarei[1], Rahbar Rahimi[1], Taleb Zarei[1], Nader Naziri[2]
[1]Chemical Engineering Department, University of Sistan and Baluchestan, Zahedan, P.OBox.98164-161, Iran, Rahimi@hamoon.usb.ac.ir
[2]Managing Director, Azar Energy Co., Tabriz, Iran, www. Azarenergy.com

Abstract
Sieve trays are widely used fractionating devices in separation and purification industries involving tray towers. According to the importance of trays, it is vital to predict lower operating range limits for such gas-liquid contacting devices. Weeping phenomenon observed in bubbling regime and occurs at low vapor flow rates. The experimental set up includes a 1.22 m diameter column with two test trays and two chimney trays. Hydraulic parameters and weeping rates were measured in sieve trays with 7.04 percent holes area. The model considers the tray's thickness and is able to calculate the dry tray pressure drop, total pressure drop, clear liquid height, froth height, and weeping rate simultaneously. Predicted results were in good agreement with the experimental data. This model is able to predict the trend of weeping even in higher rates where efficiency is reduced significantly.

Key words: sieve tray, hydrodynamic, weeping, CFD

1. Introduction

Distillation tray design is a combination of theoretical and empirical challenges. Good design lead to good phase contacts with acceptable mass transfer and efficiency, thus trays must have flexibility to operate in satisfactory region of operating conditions. Such regions called as operating windows or performance diagram of trays. The vapor and liquid rates will determine the operating window of tray. At low vapor rate trays will weep, at high rates froth touch the above upper tray and entrainment will start. Upper and lower operating limits of the trays are highly affected by these two phenomena. Since many distillation columns are operate at less than their design capacity it is important to determine weeping for trays. The dry tray pressure drop and the weep fraction are two vital hydraulic parameters that determine the lower operating limit for a tray. Tray stability is another significant characteristic that at lower vapor loads arises with oscillations and pulsations on the tray. At reduced vapor rates, weeping becomes a problem in trayed columns because it reduces tray efficiency and so adversely affects the separation achieved by the column[1-3].

Several works were done to develop relations for weeping set on and critical vapor velocity base on single holes or small perforated plates includes small diameter holes[4]. S. Fasesan[5] studied weeping in a 6.35 mm perforation plate and also a valve tray with 38.1 mm hole diameters. He has applied two methods for measure weeping from each tray on his experimental rig. Lockett et al.[6,7] claimed that in the presence of weeping, distillation tray efficiency depends on the fraction of the liquid which weeps, liquid Peclet number, stripping factor, point efficiency and the particular Lewis case. Lockett and Banik[7] have studied weeping in 3.2, 6.4, and 12.7 mm perforation plates in a large rectangular column.

Mathematical models for weeping prediction and measurement of weep rate has been developed after 1998 and the comprehensive ones that involves both sieve and valve trays belong to Wijn[8]. Zhang and Tan[9-11] tried to provide a model for bubble formation and weeping at a submerged orifice at stagnant liquid and with liquid cross flow. In recent years, the use of computational fluid dynamics (CFD) to model two phase flows in chemical engineering equipments are in great interest. This object involves trays behavior modeling since 1998[12-20]. Gesit et al.[18] and Rahimi et al.[21] developed CFD model to simulate, hydrodynamics, temperature and concentration distributions of both liquid and vapor phases and determine the point and tray efficiencies and energy efficiency. Adopting the Eulerian - Eulerian framework and solving the volume fraction and turbulence equations are also other specification of their research. the tray geometeries and operating conditions were based on the large rectangular tray of Dribika and Biddulph and FRI commercial sieve tray. Zarei et al.[22] used CFD tools for prediction of

the flow pattern and of Mini V-Grid valve (MVG) trays and compared it with sieve tray. A 3-D CFD model in the Eulerian framework was used and the simulation results showed better hydraulic behavior for MVG trays. The reviewed CFD simulations of the trays were done in the region of operation that no weeping and entrainment observed. At previous CFD works were excluded the tray thickness and the space under the tray deck from computational domain. This will be addressed in the present article. The goal of this research was to examine the CFD models ability for prediction of the trays lower operating limit in industrial scale. Also study of the sieve tray behavior at its lower operating limit is the major goal of this work. Since CFD and experimental approaches has their own restrictions individually, this study deal with coupling of the both approaches and covers their inherent limitations.

2. Experimental Approach

Figure 1 shows a schematic representation of the column used for the measurement of weeping rate. It consisted of a 1.22 m diameter column with two sieve trays (1) and two chimney trays (2). The column had three sight glasses to facilitate the observation of the phenomena occurs in the column. The tray spacing was 0.61 m. A blower (5) blows air up through the column. Water is pumped from a storage tank (10) by means of a centrifugal pump (11) into the column. The water flow rate is measured by the calibrated flowmeter (13). The water was either return to the tank or straight to drain. Since this study includes the air/water system, thus the outlet air vent to the surrounding and it is open. To uniform and calm distribution of water, the upper sieve tray inlet downcomer filled with a pall rings. The downcomer area is 0.061608 m^2. Details of trays specifications which were used are given in Table 1. Great care was taken to ensure that the trays were level and taken to seal the entire apparatus, including the blower bearings. The gas velocity was measured using a calibrated pitote tube (6) at the blower outlet. The chimney tray was located below the test tray and it collected liquid which wept from the test tray (lines 8&9in figure 1). Weeping liquid flowed from the chimney tray is collected over a given time interval after the weeping showed the steady behavior. In normal condition this stream drains to liquid storage tank. Constant weir height, downcomer clearance and tray spacing were used in the experiments. Dry tray pressure drop were measured by blocking off the clearance under the downcomers. The pressure drop of each trays measured by the manometers that were connected to the pressure taps. The pressure tap were positioned the different situation. The first at 10 cm under the tray and the second was placed 40 cm above the tray. The dynamic head of liquid on the tray was measured at two different positions. One limb of each manometer was leveled with the tray floor and the other was connected to the column wall which was connected to air space. The clear liquid height was measured by subtracting the dry pressure drop from total pressure drop at same vapor superficial velocities. The hole gas velocity used in the experiments ranged from 3 to 20 m/s. The liquid loads per weir length ranged from 30 to 60 m^3/(hr m). Data of the present work for the round commercial scale sieve tray with 7.04 percent free hole area are worth because of the lack of the hydraulics data for this type and geometry of both tray and column.

Table1. Specifications of test sieve trays

Tray diameter	Plate active area	hole area%	Number of holes	downcomer area
1.2 m	1.0078 m^2	7.04	560	0.061608 m^2
Number of sieve trays	**Hole diameter**	**Tray thickness**	**Weir height**	**downcomer clearance**
2	12.7mm	2 mm	50mm	40 mm

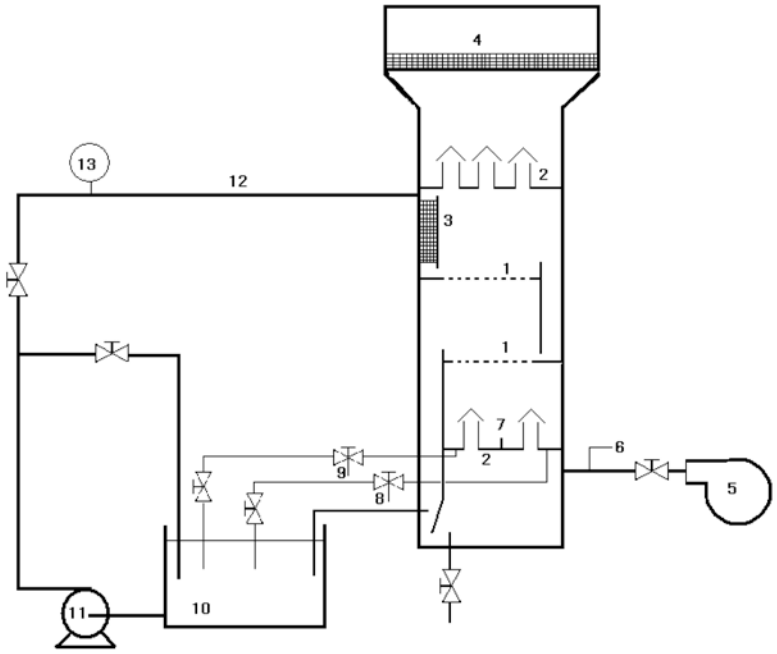

Figure 1. Experimental set-up diagram. 1, sieve trays; 2, chimney trays; 3, downcomer filled with pall ring; 4, demister pad; 5, air blower; 6, pitote tube; 7, transverse baffle; 8, upstream weeping line; 9, downstream weeping line; 10, storage tank for liquid; 11, liquid pump; 12, inlet liquid line; 13, liquid flow meter

3. CFD Approach

Two three-dimensional transient models were developed. The first one describes the dry tray and measures the dry tray pressure drop while the second model represented for two phase case or wet tray. The dispersed gas and the continuous liquid are modeled in the Eulerian framework as two interpenetrating phases having separate transport equations. The tray geometry is in commercial scale and involves actual number of holes with their circular real shapes. The time and volume averaged continuity and momentum equations are numerically solved for each phase. Assuming two computational domains interacting with each other while have different drag coefficient and some differences in hydraulic manner descriptions is another future of the developed two phase model. Upper domain includes the tray deck and tray spacing to upper tray with outlet downcomer space. Lower domain involves space beneath the tray and chimneys of chimney tray deck and plays its role for weeping liquid as a trap. Working at gas velocities that provide dominant froth regime and heterogeneous bubbly regime for lower values of gas velocity, thus the model uses Krishna[17] drag coefficient for interphase momentum exchange term in the first domain. This relation is independent of bubble diameter, and is suitable for CFD use. The turbulence viscosities were related to the mean flow variables by using the standard k-ε model. No turbulence model was considered for calculating the velocity fields within the dispersed gas phase. The slip velocity, $V_{slip} = |V_G - V_L|$, is estimated from the gas superficial velocity, **V**s For the average gas holdup fraction, Bennett et al. correlation was considered[21].

The model used a finite volume solver using body-fitted grids. The used grids is non-staggered. the pressure velocity coupling is obtained using the SIMPLE algorithm. The transient equations were solved with 0.002 s timesteps until quasi steady state was reached. The models used Upwind approach for advection descritisation scheme and second order backward Euler for the time integration. For dry tray the liquid inlet and outlet boundries are blocked off and bocomes as a parts of the wall. Because of symmetric flow fields about the tray center, only half of the tray was modeled so as to save computational time and hardware memory. The model includes the downcomer and assumes the tray thickness and space under the tray.The simulations were carried out at Eularian framework with air as a single continuous phase for the dry model. The governing equations are same as the two phase case but all of them represent for the single phase .The investigated values of F_s are at lower operating ranges.

Complicated geometry of the simulated tray uses unstructured mesh for grid generation. High ratio of tray diameter and tray spacing dimensions than holes size and tray thickness and also focusing on the dispersion height that flows on tray floors make us to use finer meshing near the tray deck and holes while larger cell are belong to the spaces where located far from the tray deck. Unlike structured grids, coordinate transformation is not performed and as a result they can be used for irregular geometries but at the expense of more complex computer programming[22]. In the unstructured meshes, it is possible to get results for the actual number of holes. By the aid of 717392 tetrahedron mesh the dry computational domain were breakdown. While other computational domain where use for wet tray case having 672457 meshes and 132316 number of nodes.A no-slip wall boundary condition was specified for the liquid phase and a free slip wall boundary condition was used for the gas phase. At the plane of symmetry, the normal component of velocity is zero and the gradient of the other variable in the transverse direction are taken to be zero. The gas and liquid that were simulated are air and water at 25 degree Celsius and at atmospheric pressure. Initially, the volume fraction of air and water in the whole of tray was specified.

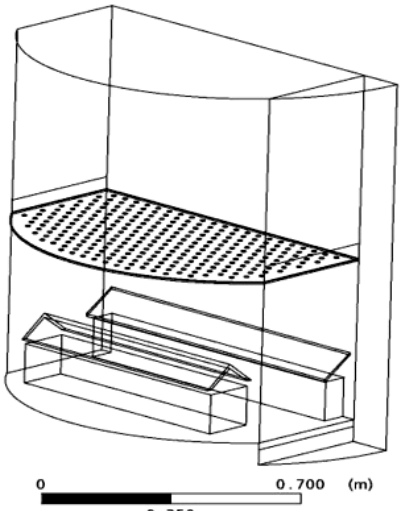

Figure 2. Simulated sieve tray

A parabolic profile is assumed for the liquid inlet velocity. The outlet specification will be in agreement with the specification of inlet where only one fluid was assumed to enter. A no-slip wall boundary condition was specified for the liquid phase and a free slip wall boundary condition was used for the gas phase. At the plane of symmetry, the normal component of velocity is zero and the gradient of the other variable in the transverse direction are taken to be zero.

4. Result and discussion

Dry tray pressure drop is a hydraulic parameter which affects the weeping occurrence. Figure 3(a) shows experimental and CFD results for the dry pressure drop as a function of the F-factor. Same trends were obtained by both approaches for dry tray pressure drop changes versus F-factor. Weeping occurs when the pressure drop of the passing vapor through the tray deck is insufficient to support the liquid. Therefore, by increase of pressure drop the liquid turndown ratio increases. Experimental work was done to record weep rate from the tray at Q_L = 30, 36.6 and 60 m^3/mh. Each liquid rate covers a range of F factor for low gas rates. The simulations were done at Q_L = 60 m^3/mh for Fs = 0.536, 0.75 and 0.95 m/s$(kg/m^3)^{0.5}$. Let the system to proceed in specified time interval passing quasi steady state conditions. The clear liquid height was calculated as the tray spacing multiplied by the volume average of the liquid volume fraction above the bubbling area of the tray floor. At the quasi-steady state condition the values of clear liquid height are approximately constant, therefore volume of weeping liquid that collected on the chimney tray was measured. This gives the average value of weeping liquid. Also, the model records the variations of weep rate with elapsed time. Figure 3(b), shows comparison between experimental and simulation results for Q_L = 60 m^3/h. Both approaches illustrate that the weeping rate increases with decreasing in gas velocity. Hence, it is

possible to predict the tray lower operating limit and gain the certain weep percent at different gas and liquid loads. Also, weep rate from upstream and downstream represents the nonuniformity on the tray through weeping condition. Figure 4(a) shows experimental results for Q_L = 36.6 m^3/m h. Upstream section of tray more weeped than the downstream section at the low and medium weeping conditions. Results shows that gas and liquid flows tend to establish channeling on tray by increasing weep rate. Figure 4(b) shows that the total pressure drop decreases by increasing the weeping rate, because of decreasing in froth height and clear liquid heights. Also, weeping leads to lower weir liquid loads.

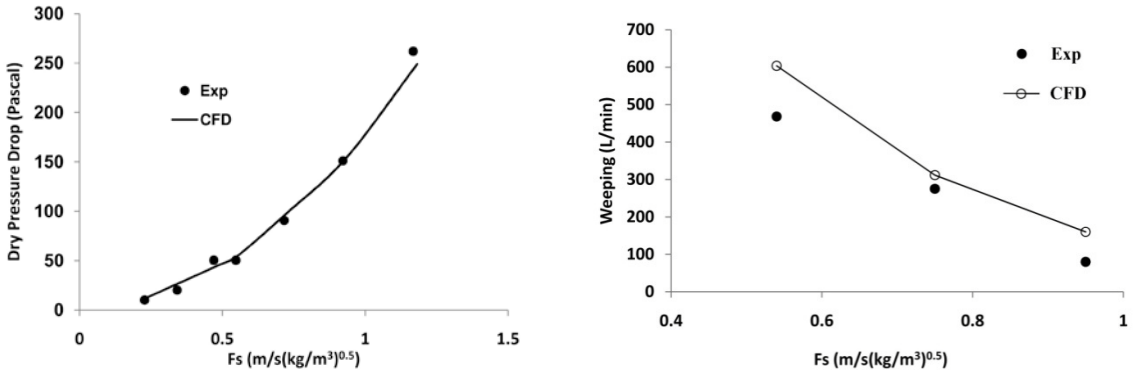

(a) **(b)**

Figure 3. a) Experimental and CFD results for the dry pressure drop,
b) Experimental and simulation results for Q_L = 60 m^3/h.

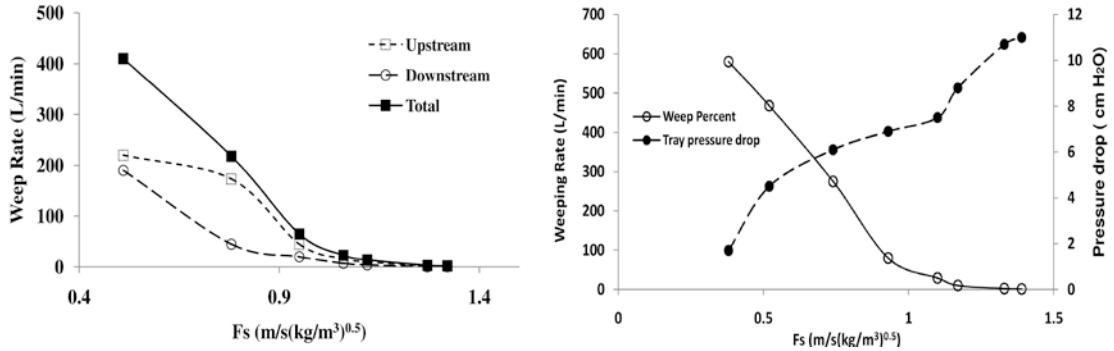

(a) **(b)**

Figure 4. a) Experimental results for Q_L = 36.6 m^3/m h,
b) Experimental results pressure drop and weeping rate for Q_L = 60 m^3/m h.

5. Conclusion

A study on the 1.2 m diameter sieve tray at weeping conditions was done by the experimental work and CFD model. Measurement of the weeping from upstream and downstream shows the intensity of no uniformity on tray. Transient 3D model was developed predict same trend for weep rate as experimental results. Also dry tray pressure drop was predicted by the single phase CFD model. Therefore it is possible to predict the sieve tray lower operating limit by CFD tools and gain deep insight around the weeping tray hydraulics changes by coupling experimental work and CFD models.

Nomenclature

F_S	[m/s(kg/m^3)$^{0.5}$]	F factor=$V_S\sqrt{\rho_G}$
Q_L	[m^3/mh]	Liquid volumetric flow rate
V_G	[m/s]	Gas phase superficial velocity
V_L	[m/s]	Liquid phase superficial velocity
V_S	[m/s]	Gas phase superficial velocity based on the bubbling area,
ρ_G	[kg/m^3]	Gas density

ReferenceS

1. M. W. Biddulph, *AIChE J*. 21 (1975) 41.
2. D. R. Summers, Sulzer Chemtech USA, Inc., AIChE Annual Austin, Texas(2004).
3. Kister H. Z., *Distillation Design,* McGraw-Hill (1992).
4. Lockett,M.J., *Distillation Tray Fundamentals*, Cambridge University Press,(1986).
5. S. O. Fasesan, *Ind. Eng. Chem. Process Des. Dev*., 24, (1985), 1073-1080.
6. M.J. Lockett, M.A. Rahman, H.A. Dhulesia, *AIChE J*., 30(1984), 423-431.
7. M.J. Lockett,S. Banik, *Ind. Eng. Process Des. Dev*., 25, (1986), 561-569.
8. E.F.Wijin , *Chem. Eng. J.,*70,(1998),143-155.
9. Wenxing Zhang, R. B. H. Tan, *Chem. Eng. Sci*. 55(2000) 6243-6250.
10. Wenxing Zhang, R. B. H. Tan, *Chem. Eng. Sci* 58(2003) 287-295.
11. Wenxing Zhang, R. B. H. Tan, *Chem. Eng. Techn*. 26, (2003), 1169-1175.
12. Mehta, B. et.al, *Chem.Eng. Res. Des., Trans. Inst. Chem. Eng*., 76, (1998), p.843.
13. Fischer, C. H., and Quarini, J. L., AIChE Meeting, Miami Beach, FL (1998).
14. 14.Yu, K. T., Yuan, X. G., You, X. Y. and Liu, C. T, *Chem. Eng. Res. Des*. 77a , (1999), 554.
15. Liu, C. J., Yuan, X. G., Yu, K. T. and Zhu, X. J., *Chem. Eng. Sci*., 55 (2000), 2287.
16. Krishna, R. et.al*, Chem. Eng. Res. Des., Trans. Inst. Chem. Eng*., 77, (1999) 639.
17. Van Baten, J. M. and Krishna, R., *Chem. Eng. J.,* 77, (2000), 143.
18. Gesit, G. K., Nandakumar, K. and Chuang, K. T., *AIChE. J*. , 49, (2003), 910.
19. Solari,. B., and R. L. Bell, *AIChE J*., 32 (1986), 640.
20. Wang, X. L., Liu, C. J., Yuan, X. G. and Yu, K. T*., Ind. Eng. Chem. Res.* 43, (2004), 2556-2567.
21. Rahimi R., Rahimi, M. R., Shahraki, F. and Zivdar, M., *Chem. Eng and Technol*. (2006), 326-335.
22. T. Zarei, R. Rahimi, M. Zivdar, *Korean J. Chem. Eng*., 26(2009), 1213-1219.